Theor Chem Acc (2017) 136:32
DOI 10.1007/s00214-017-2061-7

REGULAR ARTICLE

Singlet open-shell diradical nature and redox properties of conjugated carbonyls: a quantum chemical study

Diego López-Carballeira[1] · **Fernando Ruipérez**[1]

Received: 22 September 2016 / Accepted: 16 December 2016 / Published online: 17 February 2017

Abstract In the present work, a set of 90 conjugated carbonyls based on cyclic hydrocarbons with different ring sizes are studied by means of theoretical methods of quantum chemistry in order to analyze their singlet open-shell diradical character and its influence in different molecular properties. In particular, we have investigated the molecular structures, singlet–triplet gaps, ionization energies (IE), electron affinities (EA), first (E_1) and second (E_2) redox potentials and coordination of the reduced species to lithium cation. The diradical character is estimated using the diradical index from the spin-projected unrestricted Hartree–Fock theory (y_{PUHF}). Non-negligible diradical character is accounted for most of the studied molecules, and trends may be devised in relation to their molecular properties. Thus, in those groups where several or all molecules show certain diradical character, this feature accomplishes larger EAs, E_1 and E_2. In this study, 35 carbonyls display E_1 values greater than 3 V, and the largest calculated value is 4.22 V. Regarding the IEs, no clear relationship may be established, although in some cases with large values of y_{PUHF} small IEs are recorded. Finally, the binding energy to Li^+ mainly depends on the relative position of the carbonyls, and the lithiation process is favored when the carbonyl moieties are adjacent or close in the molecule. These results highlight the importance of the diradical character on conjugated carbonyls and its effect in molecular properties such as redox potentials, a characteristic that may be exploited both theoretically and experimentally to provide with a deeper insight on the application of these diradicals as organic cathode materials.

Keywords Singlet diradicals · Conjugated carbonyls · Redox properties · Electron affinity · Ionization energy · Cathode material

1 Introduction

The growing interest in organic singlet open-shell diradicals relies on the potential applications they show in organic electronics such as light-emitting diodes [1], field effect transistors [1, 2] and photovoltaics [3, 4]. Besides, as a consequence of small HOMO–LUMO gaps, they exhibit relevant physicochemical properties like high-yield singlet fission processes [5–7], low-lying excited states [8, 9], nonlinear optics [10] and tailorable low-spin/high-spin gaps [11]. Due to their inherent instability, diradical systems are frequently related with reaction intermediates; however, significant developments in the chemistry of open-shell molecules have made it possible to increase the lifetimes and prepare long-lived diradicals [12]. For instance, benzoquinodimethane [13] and thiophene [14] derivatives, quinoidal bisanthene [15] and indeno[1,2-*b*]fluorenes [16–18], among others, have been successfully synthesized. Although singlet diradicals have been widely investigated both experimental and theoretically [12, 19–30], there is a lack of fundamental research focused to unveil the redox

Published as part of the special collection of articles derived from the 10th Congress on Electronic Structure: Principles and Applications (ESPA-2016).

Electronic supplementary material The online version of this article (doi:10.1007/s00214-017-2061-7) contains supplementary material, which is available to authorized users.

✉ Fernando Ruipérez
fernando.ruiperez@polymat.eu

[1] POLYMAT, Joxe Mari Korta Center, University of the Basque Country UPV/EHU, Avda. Tolosa 72, 20018 Donostia – San Sebastián, Spain

behavior of these open-shell systems, a key feature for the design of new organic electrode materials. Organic systems, in general, are considered a very promising type of energy storage devices due to their unique properties, such as high energy density (product of the capacity and the working potential), flexibility, processability, sustainability and structural diversity [31].

Every organic molecule that can undergo a reversible redox reaction is a possible candidate to be an electrode material but, besides this reaction reversibility, the accomplishment of some other basic requirements is requested to improve the electrochemical performance. Thus, in order to design and evaluate new organic cathode materials, we should look for structures with both high redox potential and theoretical capacity. The former is mainly determined by the electroactive moiety and the substituents, while the latter can be increased reducing the molecular weight of the structural unit. In this manner, conjugated carbonyl compounds are encouraging candidates for energy storage materials due to their stability, possibility of shifting the formal potential by introducing modifications in the molecule, reversibility of their redox chemistry, availability from biomass and low CO_2 footprint [32–36]. Also, the combination of a large number of carbonyl groups with low molecular weights results in high-capacity electrodes. For practical use in a battery, there must be a voltage gap large enough between a cathode with higher redox potential and an anode with lower redox potential. Nowadays, the highest average potential that can be obtained using carbonyl-based cells is around 2.8 V [37] (vs. Li^+/Li electrode), still far from common inorganic cathode materials (3.5–4 V). Thus, in the pursuit of higher energy density, understanding carbonyl utilization and predictable engineering of the reduction potentials is desired.

In contrast to the case of inorganic electrode materials, a relatively low amount of fundamental studies have been conducted in order to understand the redox properties of conjugated carbonyls [38–44], although some relationships between redox voltage and properties such as electrophilicity and LUMO energy levels have already been established from theoretical studies [45, 46]. In this manner, Aspuru-Guzik et al. [47] employed a high-throughput computational approach to determine the redox potentials of a large number of quinone derivatives with different backbone lengths and functionalities. Assary et al. [48] also employed theoretical methods of quantum chemistry to investigate the first and second redox potentials of anthraquinone and quinoxaline [49] derivates. Jang and co-workers have recently investigated the fundamental redox characteristics of model quinone derivatives to be used as positive electrodes for lithium-ion batteries, in order to understand the Li-binding properties [50]. Nevertheless, we are still far from the degree of understanding regarding structure-redox activity that may be useful for a theoretically aided selection prior to experimental characterization.

Besides, we have observed in preliminary calculations that many conjugated carbonyls possess a non-negligible diradical character, and the lowest energy state corresponds to the open-shell singlet state. However, this important issue has been omitted in almost all of the published works so far. Thus, the aim of this work is to analyze the diradical nature of conjugated carbonyls and provide with a better understanding of how this characteristic may affect common properties such as molecular geometry, singlet–triplet gap, ionization energy or coordination energy of the reduced species to metal cations, as well as the electrochemical features, in pursuit of new organic compounds with high redox potentials useful as cathode materials. In order to do so, a set of ninety cyclic conjugated carbonyls has been designed and, using theoretical methods of quantum chemistry, the singlet open-shell diradical character as well as its influence on the redox chemistry, among other important properties, has been studied.

2 Computational details

2.1 Geometry optimization and diradical character

All geometry optimizations have been performed in gas phase within density functional theory (DFT) [51, 52] using the B3PW91 functional [53–55] in combination with the 6-31+G(*d*) basis set [56]. Harmonic vibrational frequencies were obtained at the same level of theory to confirm that all the structures were minima in the potential energy surfaces (no imaginary frequencies were found) and to evaluate the zero-point vibrational energy (ZPVE) and the thermal corrections to the Gibbs free energy ($T = 298$ K, 1 atm) in the harmonic oscillator approximation. Single-point calculations using the aug-cc-pVTZ basis set [57] were carried out on the optimized structures to refine the electronic energy. This level of theory has been found to be accurate for the modelization of open-shell singlet diradicals [58]. Solvent effects, in acetonitrile, have been estimated using the polarizable continuum model (PCM) approach [59–62] at the B3PW91/6-31G(*d*) level of theory, using the gas-phase geometries. In the case of those molecules whose diradical character is small, the high-level G3(MP2)-RAD composite procedure [63] has also been employed in the calculation of the singlet–triplet gap. However, its use may be limited in the calculation of delocalized radicals [64]. All these calculations have been carried out using the Gaussian 09 package [65].

The open-shell singlet state energies have been obtained by means of the broken-symmetry formulation [66–68], in which the wavefunctions are no longer eigenfunctions of

the $\langle \widehat{S}^2 \rangle = \langle S(S+1) \rangle$ operator. For a triplet state, the value of this operator is 2 and for a closed-shell singlet is 0. However, in the broken-symmetry solution we look for $\langle \widehat{S}^2 \rangle = 1$, which is not a pure spin state and the wavefunction is an approximate mixture of the closed-shell singlet and the triplet wavefunctions, stated in computational chemistry as spin contamination. The singlet diradical character is estimated using the diradical index (y_{PUHF}) from the spin-projected unrestricted Hartree–Fock (PUHF) theory [69–71], using the aug-cc-pVTZ basis set, as:

$$y_{\mathrm{PUHF}} = 1 - \frac{2T}{1+T^2}$$

where T is defined as the orbital overlap and is calculated using the occupation number (n) of the UHF natural orbitals:

$$T = \frac{n_{\mathrm{HOMO}} - n_{\mathrm{LUMO}}}{2}$$

An index value of 1 states for a perfect diradical, while a value of 0 means a closed-shell singlet. For the correct description of the single-state energies, the spin contamination must be corrected and, to do that, the approximation of Yamaguchi [72, 73] is particularly useful:

$$J = \frac{E_{\mathrm{BS}} - E_{T(\mathrm{BS})}}{\left\langle \widehat{S}^2_{T(\mathrm{BS})} \right\rangle - \left\langle \widehat{S}^2_{\mathrm{BS}} \right\rangle}$$

where J is the electron magnetic exchange interaction and $E_{\mathrm{BS}} - E_{T(\mathrm{BS})}$ is the vertical excitation energy. J is related to the singlet–triplet gap as follows:

$$\Delta E_{ST}^{\mathrm{vert}} = E_S - E_T = 2J$$

and, to estimate the adiabatic energy, the following expression is used:

$$\Delta E_{ST}^{\mathrm{adiab}} = E_{\mathrm{BS}} - E_{T(T)} = 2J + E_{T(\mathrm{BS})} - E_{T(T)}$$

where $E_{T(\mathrm{BS})}$ is the energy of the triplet state in the broken-symmetry geometry of the singlet state and $E_{T(T)}$ is the energy of the triplet in its optimized geometry.

2.2 Electron affinities, ionization energies and reduction potentials

Electron affinities, ionization energies and reduction potentials are calculated at the B3PW91/aug-cc-pVTZ//B3PW91/6-31+G(*d*) level of theory. The G3(MP2)-RAD composite method has also been employed in those molecules with mainly closed-shell character, since it has been shown to be an accurate method for the calculation of electron affinities and redox potentials of quinone derivatives [38]. The reduction potentials have been calculated using the thermodynamic cycle shown in Fig. 1, where the Gibbs free energy of the reduction half-reaction, $\Delta G^{\mathrm{RED}}_{(\mathrm{solv})}$, consists of the free energy change in the gas phase and the solvation free energies (in acetonitrile) of the oxidized and reduced species.

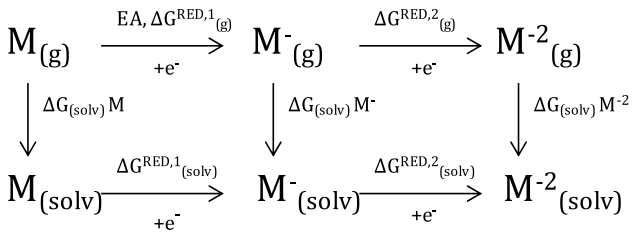

Fig. 1 Thermodynamic cycle used in the calculation of the first (E_1) and second (E_2) redox potentials

$$\Delta G^{\mathrm{RED}}_{(\mathrm{solv})} = \Delta G^{\mathrm{RED}}_{(g)} + \Delta G_{(\mathrm{solv})}M^{-} - \Delta G_{(\mathrm{solv})}M$$

The relation between the Gibbs energy and the electrode potential (E) of a half-cell is:

$$E = -\frac{\Delta G}{nF} - E_{\mathrm{ref}}$$

where F is the Faraday constant (96,485 C/mol) and n is the number of electrons in the half-reaction, with the substraction of the reduction potential of the reference electrode. In this work, we have used the reference value −1.24 V, which represents the difference between the standard hydrogen electrode (SHE, −4.28 V) [74] and the Li/Li^+ redox couple (−3.04 V). We have also used the reference value −4.67 V, corresponding to the saturated calomel electrode (SCE), in order to compare with the available experimental results.

2.3 CASSCF/CASPT2 calculations

In order to assess some parameters and to have a deeper insight into the electronic structure of particular molecules, some single-point calculations have been performed at the CASPT2/aug-cc-pVTZ level of theory. The active space in the CASSCF calculations [75–77] is defined by the π bonding and antibonding molecular orbitals. Using this wavefunctions, CASPT2 calculations [78, 79] are carried out to include the dynamic correlation effects. The MOLCAS 8.0 suite of programs [80] was used in all the wavefunction-based calculations.

2.4 Aromaticity

The GIAO method [81, 82] has been used, at the B3PW91/6-311++G(*d*,*p*) level of theory, to perform calculations of NICS (nuclear independent chemical shift) [83] at 1 Å above the center of the ring (NICS(1)), in order to better estimate

the effects of the π-electron ring current while the σ-bonding contributions are diminished [84, 85]. The NICS data are reported as the negative value of the absolute isotropic magnetic shielding, following the NMR chemical shift conventions, where negative NICS values (magnetically shielded) indicate aromaticity while positive values (magnetically deshielded) and values close to zero indicate antiaromaticity. Additionally, we have calculated the anisotropy of magnetic susceptibility, $\Delta\chi$, which can be used as an experimental measure of aromaticity [86], and is defined as:

$$\Delta\chi = \chi_{ZZ} - \frac{(\chi_{XX} + \chi_{YY})}{2}$$

where χ_{ZZ} is the magnetic susceptibility component corresponding to the axis normal to the molecule, while χ_{XX} and χ_{YY} are the in-plane components. Analogously to NICS(1) index, negative values of $\Delta\chi$ denote aromatic character.

3 Results and discussion

A set of 90 carbonyls formed by one, two or three fused rings with sizes between three and seven carbons has been designed. The full set of molecules is available in Fig. 1 of the Supporting Information (SI). All molecules contain one or two carbonyl groups in order to enable double-bond conjugation in the rings. All compounds are labeled using the following nomenclature: *n*,*m*-C($x + y + z$), where *n* and *m* refer to the positions of the carbonyl groups, and *x, y* and *z* the size of each ring, in increasing order. In Fig. 2 are displayed some representative molecules of each class.

In the next sections, the results are presented and organized as follows: firstly, we analyze the diradical character and the singlet–triplet gaps (STG) and their connection with the geometrical features, relative stability and aromaticity. Next, electron affinities (EA), ionization energies (IE), as well as first and second redox potentials (E_1 and E_2) are discussed. Finally, the complexation energy with Li^+ is studied, in an attempt to compare with the redox reactions that carbonyl compounds undergo in lithium-ion batteries. All these properties are discussed in terms of the diradical nature of the ground state as well as the structural variations among different molecules, such as the size and number of rings, or the relative arrangement of the carbonyls.

3.1 Diradical character and singlet–triplet gaps

In Fig. 3, the diradical character (y_{PUHF}) and singlet–triplet gaps (STG) for all molecules are displayed. The numerical values are collected in Tables S1 and S2, respectively, in the SI. It is observed that monocycles (1-C3, *n*,*m*-C4, 1-C5, *n*,*m*-C6 and 1-C7) are basically closed-shell

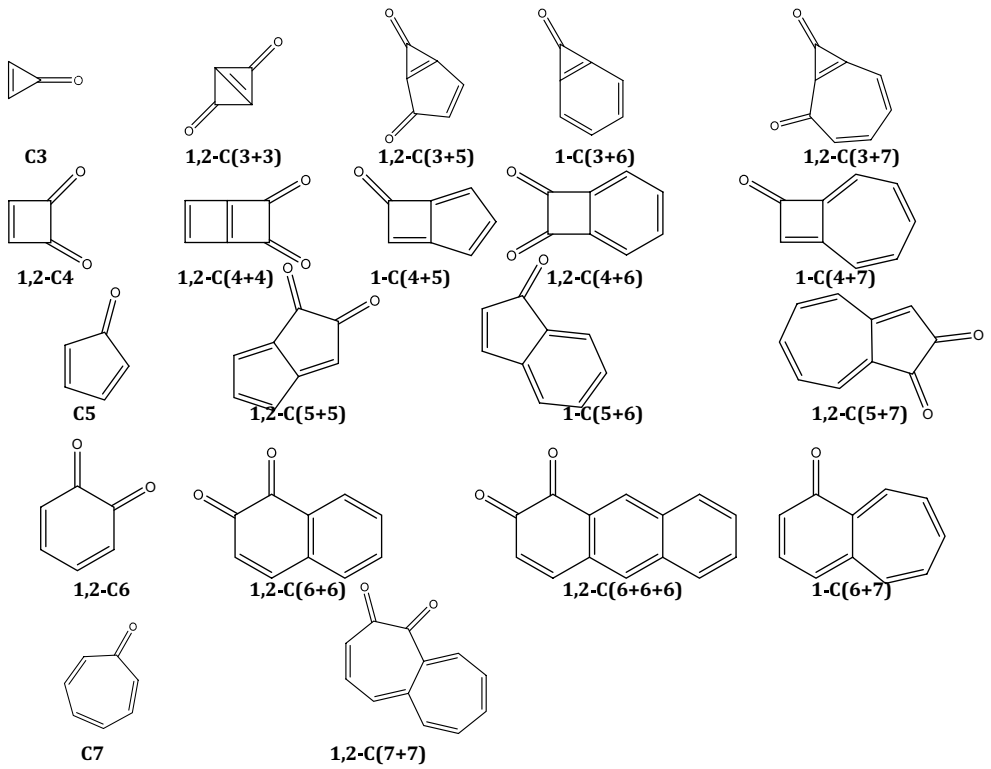

Fig. 2 Representative molecules of each group of carbonyls studied in this work

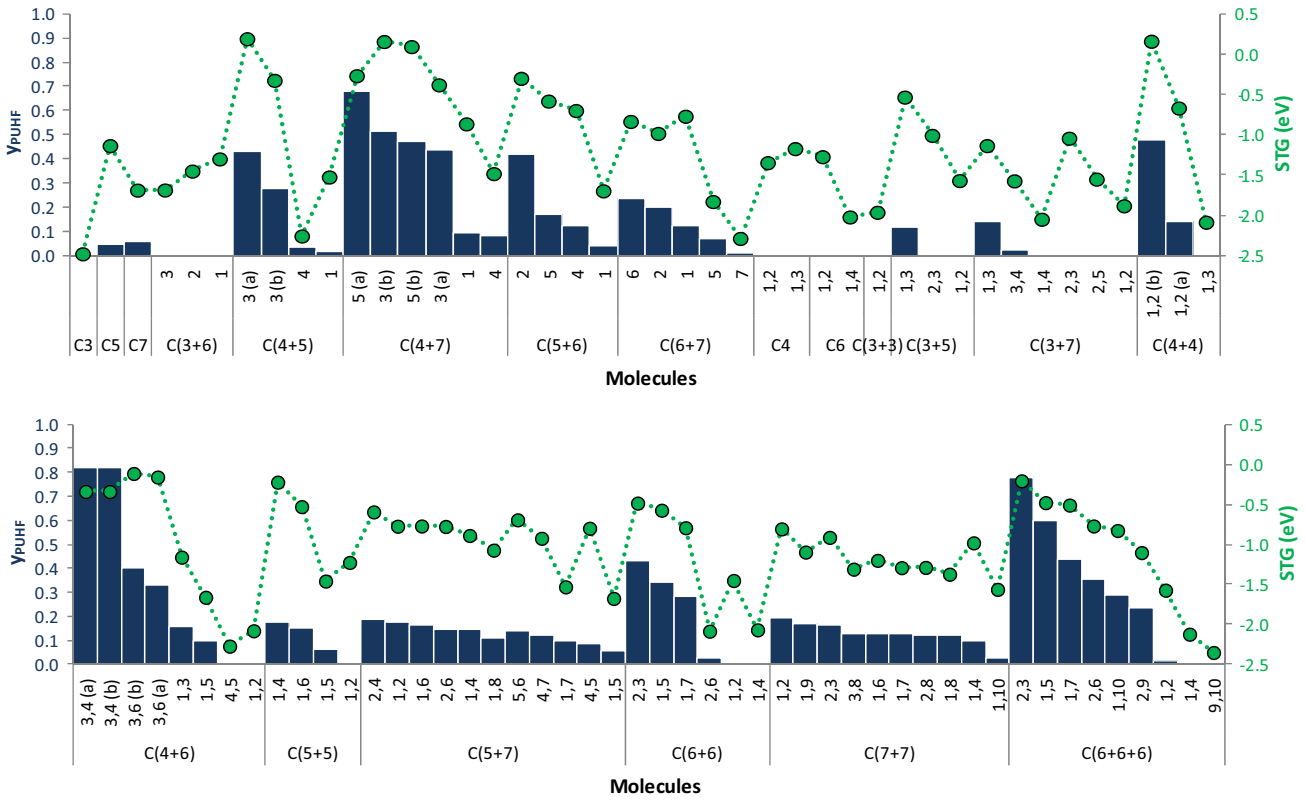

Fig. 3 Diradical character (y_{PUHF}) and adiabatic singlet–triplet gaps (STG), in eV, calculated at the B3PW91/aug-cc-pVTZ//B3PW91/6-31+G(*d*) level of theory

molecules, although an almost negligible diradical character is observed in the monocarbonyls 1-C3, 1-C5 and 1-C7. Similarly, all bicycles containing a three-membered ring are closed-shell species, with a slight diradical character observed in 1,3-C(3 + 5) and 1,3-C(3 + 7).

For the cyclobutadiene-based molecules, since cyclobutadiene is not aromatic, the relative position of the double bonds gives rise to energetically and structurally different isomers with different diradical character: (a) with a double bond linking the shared carbons of the two rings and (b) with each shared carbon having a double bond. The only exception is 3,4-C(4 + 6), where (a) and (b) isomers are equal when broken symmetry is used (see Figure S2 in the SI). In general, bicycles including cyclobutadiene show remarkable diradical character: 3(a)-C(4 + 5), 3(a,b)-C(4 + 7), 5(a,b)-C(4 + 7), 1,2(b)-C(4 + 4), 3,4(a,b)-C(4 + 6) and 3,6(b)-C(4 + 6), with $y_{PUHF} \geq 0.40$, mostly those fused to six- and seven-membered rings. Molecules containing five-membered rings show small diradical character, with $y_{PUHF} \leq 0.20$, except 1-C(5 + 6) with $y_{PUHF} = 0.42$. Up to three molecules with two benzene rings [naphthoquinones: 1,5-, 1,7- and 2,3-C(6 + 6)] and up to six molecules with three benzene rings [anthraquinones: 1,5-, 1,7-, 1,10-, 2,3-, 2,6- and 2,9-C(6 + 6 + 6)] show remarkable diradical character. Finally, bicycles with two seven-membered rings show small diradical character.

It has been previously observed that the number of fused benzene rings in oligoacenes increases the diradical character [87, 88]. However, this behavior becomes evident from pentacene and, therefore, in our study is not possible to observe it, that is, comparing y_{PUHF} values for 1,2-C6, 1,2-C(6 + 6) and 1,2-C(6 + 6 + 6), for example. Likewise, the size of the ring does not seem to be a key parameter; the diradical character of 1-C3 is $y_{PUHF} = 0$ while for 1-C7 is $y_{PUHF} = 0.06$. Thus, it seems that one of the main reasons to show diradical character is the relative position of the carbonyl moieties (in dicarbonyls) although is not possible to devise a clear trend.

The singlet–triplet energy gap (STG) is a relevant parameter to study in these systems since it provides information about the interaction between the two radical orbitals and is essential for understanding the diradical character. The magnitude of the STG is related to the electron exchange interaction (*J*), which is proportional to the overlap integral of the two molecular orbitals. When this overlap is small, the Hund's rule, which favors the triplet ground-state spin multiplicity, may not apply to diradicals. This feature can be observed in Fig. 3, where molecules with large diradical

character show small negative STGs, that is, singlet ground states. For instance, 2,3-C(6 + 6 + 6) (−0.20 eV), 5(a)-C(4 + 7) (−0.26 eV), 2-C(5 + 6) (−0.30 eV), 3,4(a,b)-C(4 + 6) (−0.34 eV), 1,5-C(6 + 6 + 6) (−0.47 eV) or 2,3-C(6 + 6) (−0.48 eV). Groups like *n*,*m*-C(5 + 7) or *n*,*m*-C(7 + 7) also display rather small STGs, yet an almost negligible diradical character. Comparing with the scarce available experimental data [89–91], a non-negligible uncertainty is observed in the B3PW91 calculations (MAE = 0.38 eV, see Table S2 and Figure S3 in the SI) and, as a consequence, some molecules can be wrongly represented with a triplet ground state. For this reason, the G3(MP2)-RAD composite method was also employed, yielding to more accurate results (MAE = 0.18 eV); however, its use may be limited in molecules with a strong diradical character and the results have to be handled with care.

The nature of the diradical can be studied by means of the variation of the density from the closed-shell to the open-shell structures (Fig. 4) and in the alpha and beta spin densities (Figure S4 in the SI). The main shift of the spin density takes place in the carbon rings, among the adjacent double bonds, especially on four-membered rings. Six-membered rings also show noticeable electronic distortions, mainly on those cases where are combined with four-membered rings. This behavior is less pronounced as the number of six-membered rings increases (naphthoquinones and anthraquinones).

3.2 Molecular geometries, stability and aromaticity

Since the geometry optimization is performed using the broken-symmetry approximation, every molecule is allowed to distort its closed-shell structure to an open-shell one, lowering the energy. Nevertheless, these changes on the structures are small and only noticeable on few structures with $\langle S^2 \rangle \neq 0$, see Figure S5 in the Supporting Information. It is observed that the C=O bond is likely to be elongated in the open-shell state. However, this variation is very small (<0.01 Å), highlighting that the unpaired

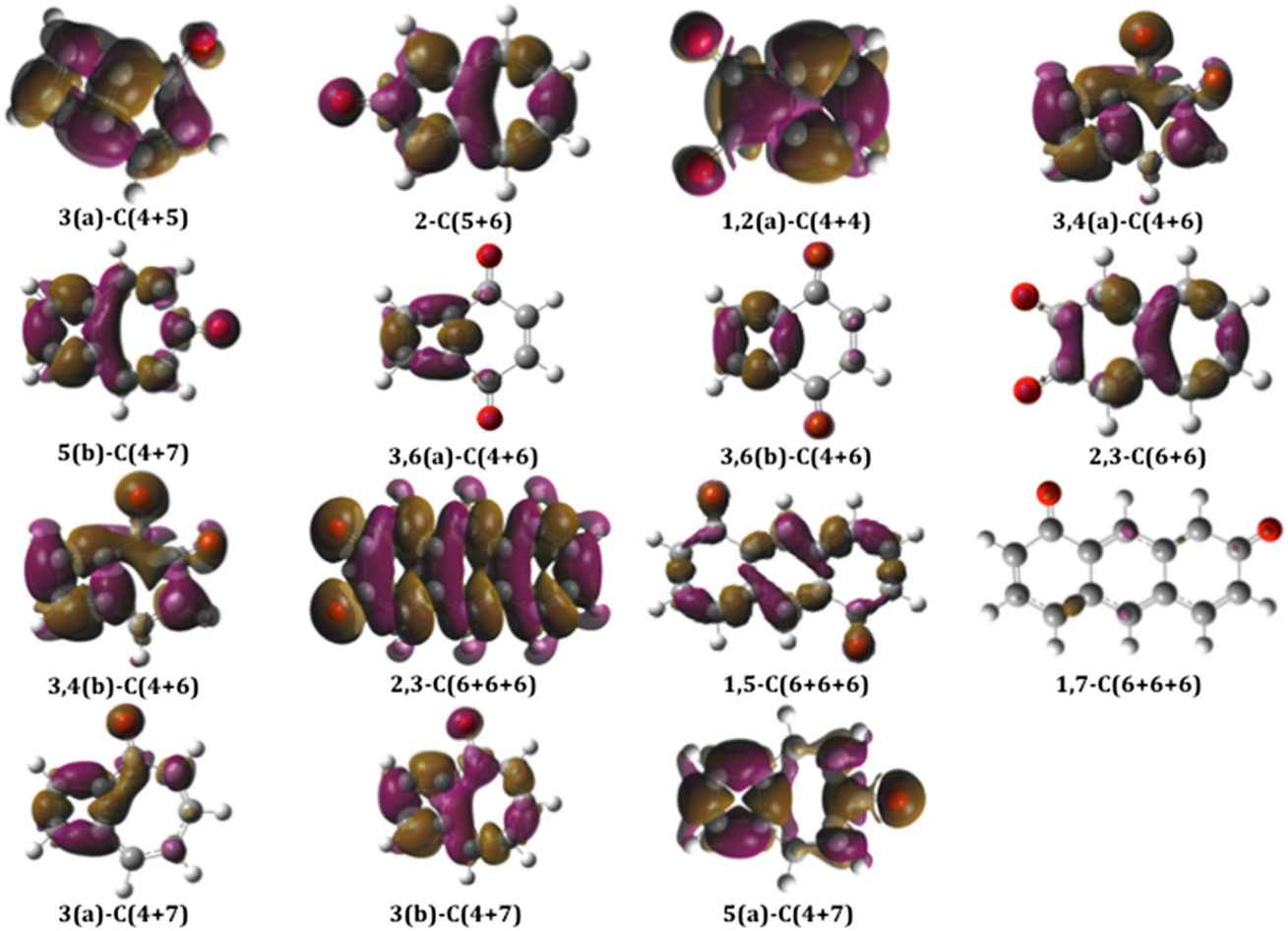

Fig. 4 Variation of the electron density (isovalue = 0.00015) from the closed-shell to the open-shell electronic structures. *Purple color* indicates regions that gain density, while *brown color* denotes loss

electrons are mainly delocalized along the carbon backbone. As it was mentioned in the previous section, the cyclobutadiene-based molecules show two energetically different isomers, (a) and (b), regarding the relative position of the double bonds. In order to confirm this results, the energy differences between these isomers have also been calculated at the CASPT2 level of theory (see Table 1), and a better agreement is observed with the broken-symmetry DFT calculations.

The diradical character in these molecules may be related to their stability. Comparing the relative energies among isomers in every group of molecules, see Fig. 5, it is observed that a greater diradical character implies a more energetical isomer.

This trend is in agreement with previously published theoretical data [92–96], and it is also reflected in the aromaticity, which provides us with a deeper insight into the ring-size effect. In order to analyze this, we have used the anisotropy of the magnetic susceptibility ($\Delta\chi$), which can be used as an experimental measure of aromaticity [86], and also the NICS criterion, since it is a useful indicator of aromaticity [97]. In Fig. 6, the calculated $\Delta\chi$ together with the diradical character is represented (the numerical values of the whole set are collected in Table S3, in the SI). Thus, although it is not straightforward to devise a clear tendency, a general decrease in the aromaticity (shift to positive values) is observed with the increase in the diradical character.

This behavior may be explained as a combination of two factors: Firstly, as it was stated in the previous section, the diradical character implies a delocalization of the spin density into the carbon backbone, diminishing their aromaticity, and, secondly, the disposition of the carbonyl moieties in the rings, which may lead to a less conjugated molecule and, therefore, decreasing the aromaticity. For instance, within the *n*,*m*-C(6 + 6 + 6) group, 2,3-C(6 + 6 + 6) shows the largest diradical

Table 1 Energy differences between (a) and (b) isomers of the cyclobutadiene derivatives, in eV, calculated at the CASPT2/aug-cc-pVTZ//B3PW91/6-31+G(*d*) and both restricted and unrestricted B3PW91/aug-cc-pVTZ//B3PW91/6-31+G(*d*) levels of theory

	CASPT2	UB3PW91	RB3PW91
1,2-C(4 + 4)	−1.28	−1.18	−1.43
3-C(4 + 5)	0.42	0.72	0.80
3,4-C(4 + 6)	0.00	0.00	0.17
3,6-C(4 + 6)	−0.02	−0.05	−0.05
3-C(4 + 7)	−0.59	−0.58	−0.75
5-C(4 + 7)	−0.23	−0.37	−0.41

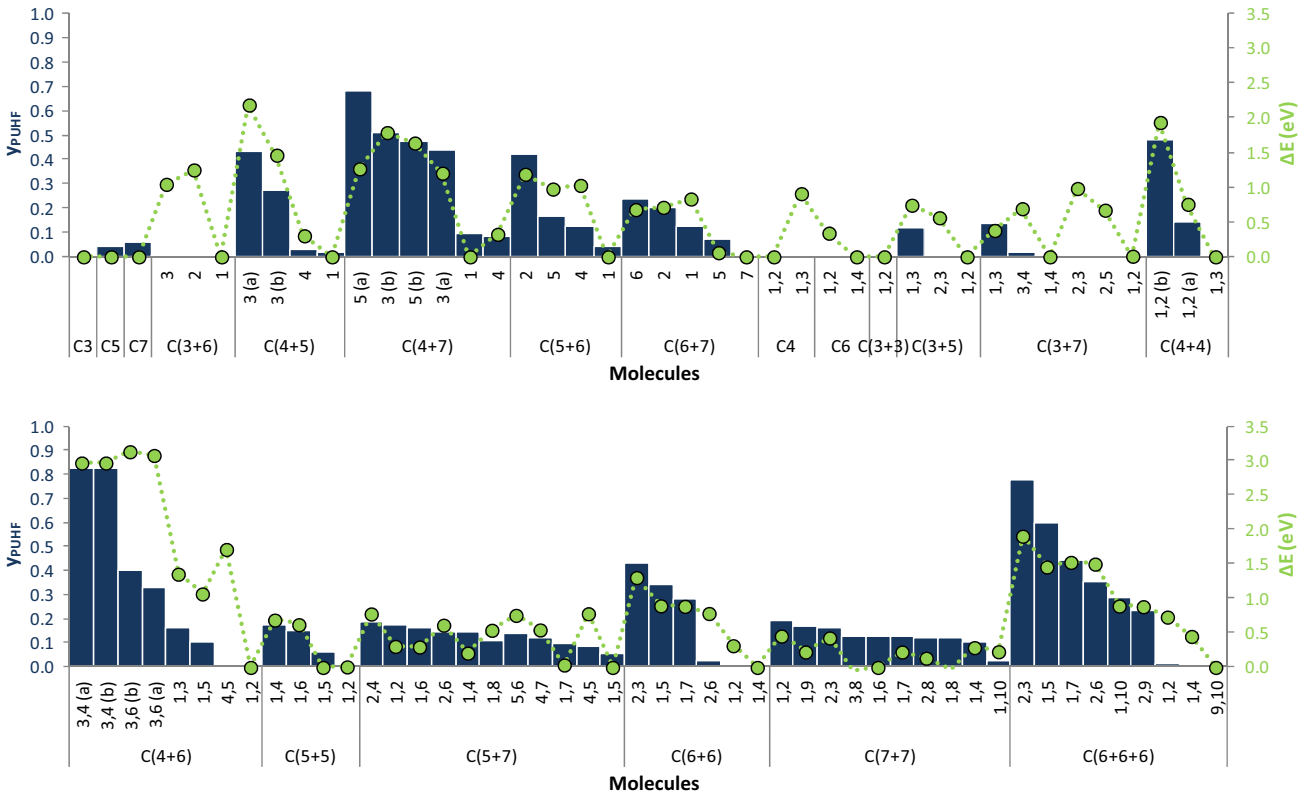

Fig. 5 Relative energies (ΔE), in eV, with respect to the lowest energy isomer, within each group of molecules

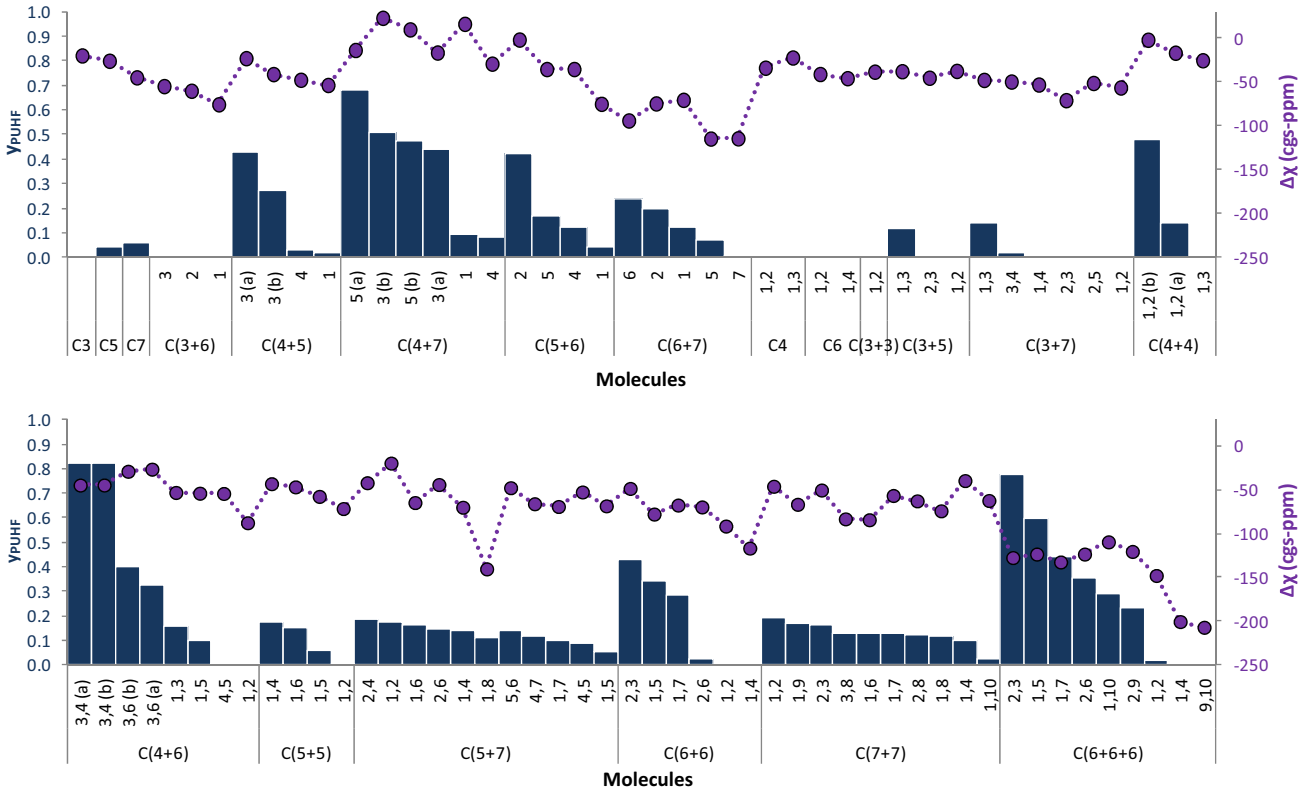

Fig. 6 Anisotropy of the magnetic susceptibility ($\Delta\chi$), in cgs-ppm, and diradical character (y_{PUHF}) calculated at the B3PW91/6-311++G(*d*,*p*)//B3PW91/6-31+G(*d*) level of theory

character, but is more aromatic ($\Delta\chi = -127.4$ cgs-ppm) than 1,10-C(6 + 6 + 6) ($\Delta\chi = -109.4$ cgs-ppm) and 2,9-C(6 + 6 + 6) ($\Delta\chi = -120.4$ cgs-ppm), due to the disposition of the carbonyls in the rings. The same can be observed in the *n*-C(4 + 7) group, where the molecule with the largest diradical character, 5(a)-C(4 + 7), is more aromatic than, for example, 1-C(4 + 7) ($\Delta\chi$ values of −14 and 15.8 cgs-ppm, respectively), which shows a very small diradical character. However, inspecting the *n*-C(5 + 6) group, both 2-C(5 + 6) and 5-C(5 + 6) possess the same degree of conjugation, but the former, which has a larger diradical character, is less aromatic ($\Delta\chi = -2.1$ cgs-ppm) than the latter ($\Delta\chi = -35.8$ cgs-ppm). In this case, the main factor affecting the aromaticity is the diradical character. Likewise, molecules such as 3(a)-C(4 + 5) ($\Delta\chi = -23.3$ cgs-ppm), 1,2(b)-C(4 + 4) ($\Delta\chi = -2.3$ cgs-ppm) or 2,3-C(6 + 6) ($\Delta\chi = -48.4$ cgs-ppm) show the most positive values of $\Delta\chi$ and the largest diradical character within their groups.

A similar analysis may be performed using the NICS(1) values (Table S4 in the SI); nevertheless, since it is a local aromaticity index, their interpretation is less straightforward in molecules with more than one ring. Following Hückel's rule [98] for aromaticity in planar rings, 1-C3 and 1-C7 molecules are aromatic [NICS(1) values of −9.48 and −2.36, respectively], while 1-C5 is antiaromatic [NICS(1) = 4.03]. However, the $\Delta\chi$ value for 1-C5 (−26.3 cgs-ppm) indicates more aromaticity than 1-C3 ($\Delta\chi = -20.2$ cgs-ppm), although both values are very close. In the monocycles with two carbonyl groups, 1,2-C4 is aromatic [NICS(1) = −3.64], while *n*,*m*-C6 is antiaromatic [NICS(1) values of 0.94 and 1.63 for *n*,*m* = 1.2 and 1.4, respectively], in contrast to the case of cyclobutadiene and benzene.

3.3 Electron affinities and ionization energies

In Fig. 7, the electron affinities (EA) and the y_{PUHF} values are represented. The only available experimental data [89, 99] correspond to molecules that have a closed-shell ground state ($y_{PUHF} = 0$). DFT calculations overestimate the experimental values around 0.3 eV, an uncertainty that may be due partly to the self-interaction error [100], which is the spurious interaction of an electron with itself, arising from the use of approximate exchange functionals. More accurate EAs have been obtained with the G3(MP2)-RAD composite method (with an average error of only 0.04 eV, see Fig. S6 in the SI), but due to its limited application in

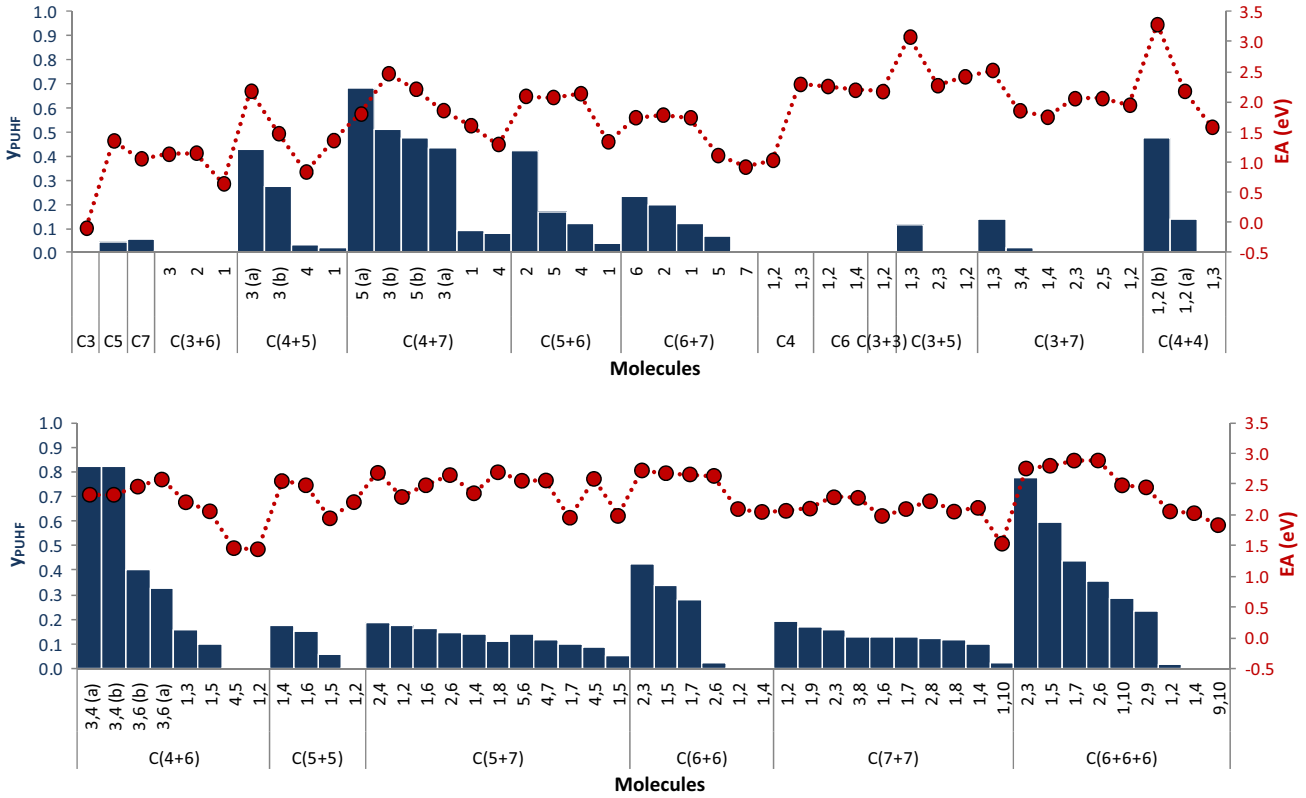

Fig. 7 Electron affinities (EA), in eV, and diradical character (y_{PUHF}) calculated at the B3PW91/aug-cc-pVTZ//B3PW91/6-31+G(*d*) level of theory

molecules with strong diradical character, and also due to convergence problems encountered in several molecules, we will only discuss the results obtained with the B3PW91 functional.

A trend in the electron affinities may be devised in several groups of molecules such as *n*-C(4 + 5), *n*-C(4 + 7), *n*-C(5 + 6), *n*-C(6 + 7), *n*,*m*-C(4 + 4), *n*,*m*-C(4 + 6), *n*,*m*-C(5 + 5), *n*,*m*-C(6 + 6) or *n*,*m*-C(6 + 6 + 6), where larger y_{PUHF} values correspond to larger EAs. However, this trend is not clear in groups where molecules are closed-shell singlets or in others with moderate (or small) diradical character, such as *n*,*m*-C(5 + 7) and *n*,*m*-C(7 + 7), a feature that can be ascribed to distortions in the molecular geometry of the anion with respect to the neutral molecule. Monocarbonyl compounds show EAs between −0.09 and 2.47 eV, while dicarbonyl EAs range from 1.03 to 3.28 eV (see the numerical values of the whole set in Table S5 of the SI). The highest value among all the molecules considered corresponds to 1,2(b)-C(4 + 4), with an EA of 3.28 eV, a molecule that shows a remarkable diradical character ($y_{PUHF} = 0.48$). Large affinities are also calculated for groups such as *n*,*m*-C(6 + 6) or *n*,*m*-C(6 + 6 + 6). The observed trend in the EAs may be explained in terms of the HOMO–LUMO gap (see Table S6 and Figure S7 in the SI), which is small in molecules with a remarkable diradical character [9, 101–103], mainly due to low-energy LUMO levels and, therefore, more likely to accept an electron. In this manner, the smallest HOMO–LUMO gaps are calculated for molecules such as 2,3-C(6 + 6 + 6) (2.22 eV), 1,5-C(6 + 6 + 6) (2.28 eV), 2,3-C(6 + 6) (2.36 eV), 3(b)-C(4 + 7) (2.35 eV) or 2-C(5 + 6) (2.42 eV), with pronounced diradical characters. Similarly, large gaps are found for closed-shell molecules, such as 1,3-C4 (5.53 eV), 1-C(3 + 6) (4.79 eV), 1,3-C(4 + 4) (4.63 eV) or 9,10-C(6 + 6 + 6) (4.13 eV).

Analogously, we have calculated the ionization energies (IE), which are gathered in Fig. 8 together with the y_{PUHF} values. All the calculated and the available experimental data [104–108] are listed in Table S7 in the SI. In this case, both DFT and G3(MP2)-RAD calculate the IEs with similar accuracy (see Figure S8 in the SI). Monocarbonyl IEs range from 6.98 to 9.35 eV, while dicarbonyl IEs range from 6.60 to 10.88 eV, much higher than the EA values. While for the electron affinities a certain correlation with the diradical character is found within particular groups, the case of the ionization energies is less clear. Still, it is possible to observe that higher diradical characters correspond to lower IEs in groups such as *n*-C(4 + 5), *n*-C(5 + 6),

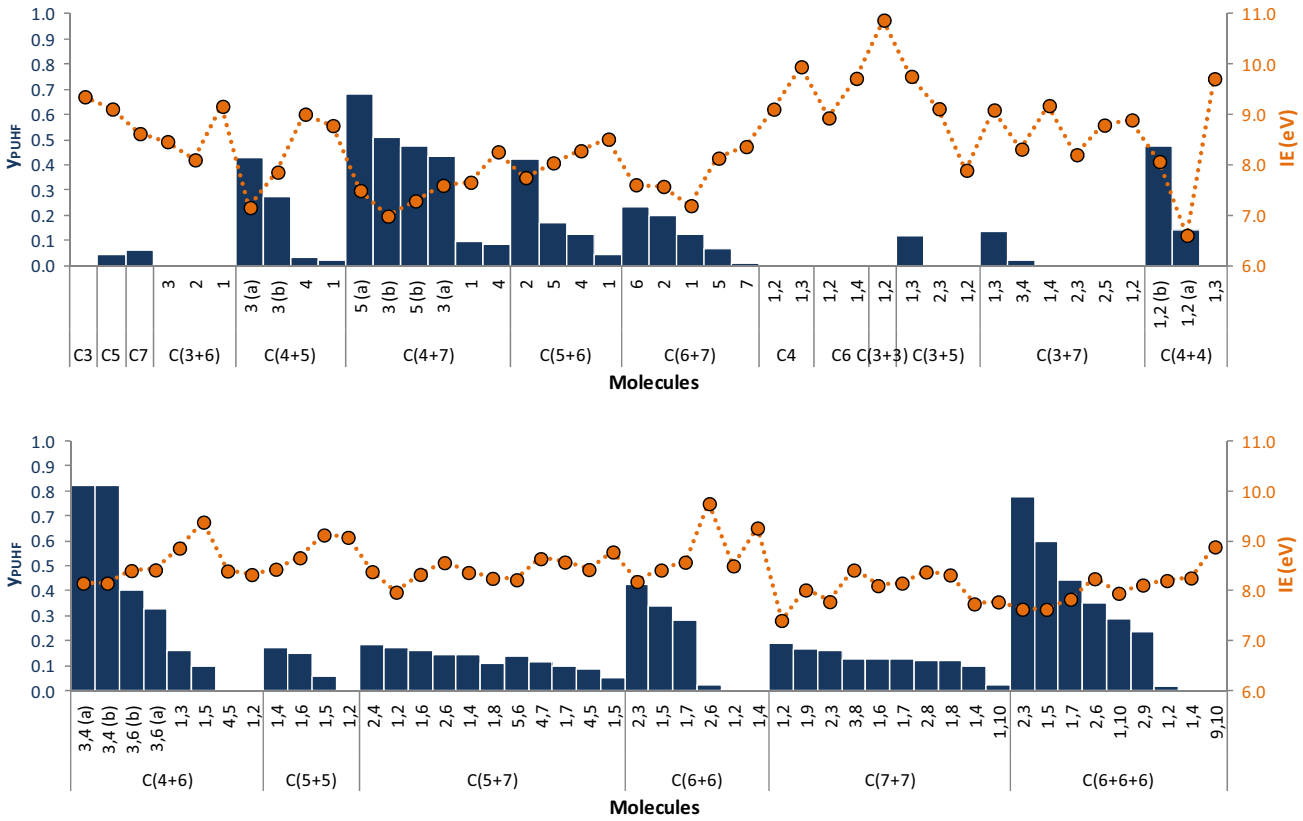

Fig. 8 Ionization energies (IE), in eV, and diradical character (y_{PUHF}) calculated at the B3PW91/aug-cc-pVTZ//B3PW91/6-31+G(*d*) level of theory

n,*m*-C(4 + 6), *n*,*m*-C(6 + 6) or *n*,*m*-C(6 + 6 + 6). Besides, in Fig. 8 and Table S7, some correlation is found between the number of fused rings and the IEs, which decrease as the number of fused rings increases. For example, the IEs of 1,2-C6, 1,2-C(6 + 6) and 1,2-C(6 + 6 + 6) are 8.93, 8.51 and 8.22 eV, respectively. Nevertheless, we have only considered molecules with up to three fused rings, and therefore, this is probably not enough to extrapolate the results to larger molecules. A similar trend is found regarding the size of the ring: Bigger rings show smaller IEs (e.g., comparing monocarbonyl 1-C3, 1-C5 and 1-C7 or dicarbonyl *n*,*m*-C4 and *n*,*m*-C6). Finally, the behavior of the IEs is similar to that of the HOMO–LUMO gaps, as expected, and smaller values are found for those carbonyls with larger diradical character.

3.4 Redox potentials and coordination to Li^+

In Fig. 9, the first reduction potentials (E_1) and the y_{PUHF} values are collected. In the Supporting Info, in Table S8, are gathered the calculated values of all molecules together with the available experimental data [109, 110]. Opposite to what was observed for the electron affinities, the first redox potentials are calculated more accurately with DFT (MAE = 0.05 V) than with G3(MP2)-RAD (MAE = 0.22 V), see Fig. S9 in the SI, which suggests that the inclusion of the solvation effects in the composite method may be problematic. The E_1 values for monocarbonyls range from 1.05 to 3.32 V, while for dicarbonyls range from 2.02 to 4.22 V. The highest value calculated in this work, 4.22 V, corresponds to 1,2(b)-C(4 + 4), which also shows the highest electron affinity (3.28 eV) and a notable diradical character (y_{PUHF} = 0.48). This redox potential is considerably higher than the usual values for carbonyl-based materials (less or around 3 V) and comparable (or even greater) to common inorganic cathode materials. There are 35 molecules that show redox potentials greater than 3 V.

Inspecting Fig. 9, we find the following general trend: Molecules with higher diradical character, within a particular group, possess higher reduction potentials, the same correlation observed in the EAs, as expected. However, in some groups, molecules with absence or low diradical character may show large reduction potentials as well, such as 1,2- and 1,4-C6, for example, with 3.19 and 3.04 V, respectively. This general trend is particularly clear in the following groups: *n*-C(4 + 5), *n*-C(4 + 7) with the exception of 5(a)-C(4 + 7), *n*-C(6 + 7), *n*,*m*-C(4 + 4),

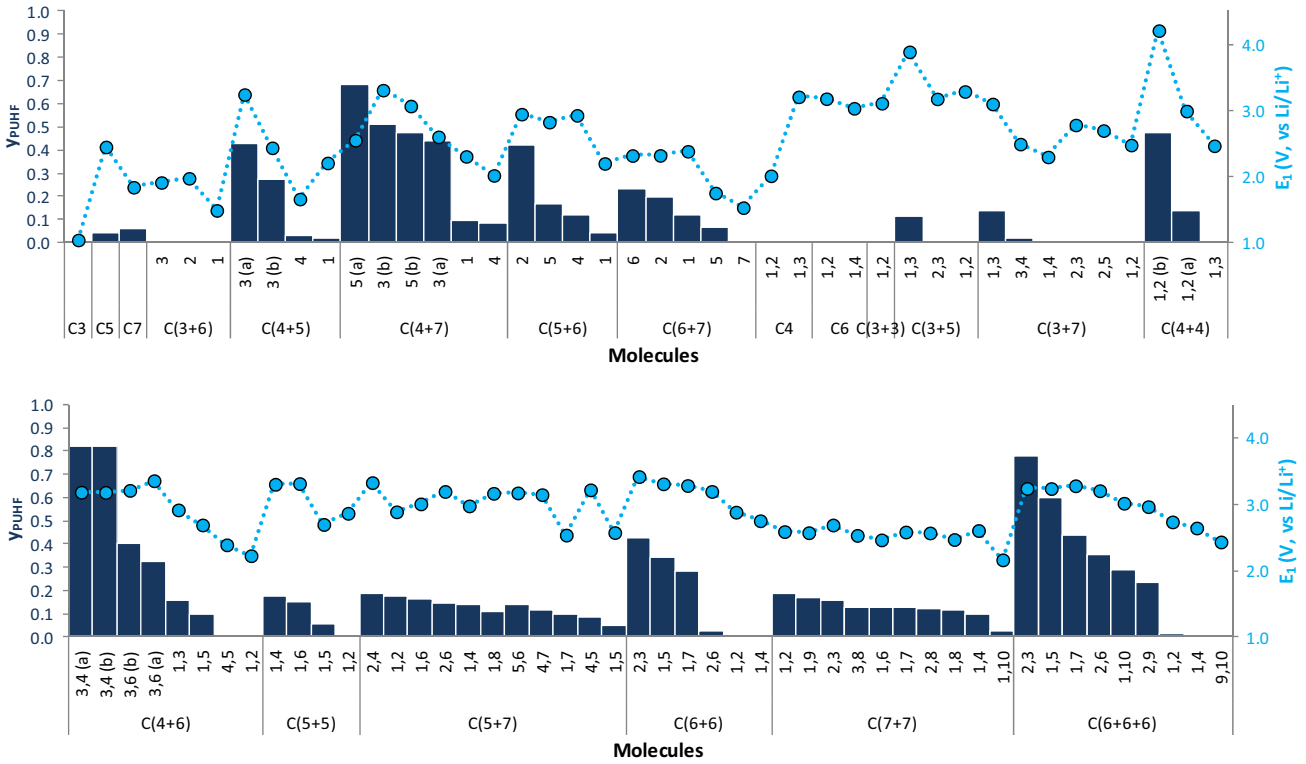

Fig. 9 First redox potentials (E_1), in V, and diradical character (y_{PUHF}) calculated at the B3PW91/aug-cc-pVTZ//B3PW91/6-31+G(*d*) level of theory

n,*m*-C(4 + 6) except 3,6(a)-C(4 + 6), *n*,*m*-C(5 + 5), *n*,*m*-C(6 + 6) and *n*,*m*-C(6 + 6 + 6). A somewhat irregular behavior is observed in *n*-C(5 + 6), *n*-C(5 + 7) and *n*,*m*-C(7 + 7). Thus, in view of these results, the effect of the diradical character may be a new, unexplored variable for tuning the redox potential in the design of new organic cathode materials. Besides the diradical character, the size of the ring and the number of fused rings may also affect the redox potential. We observe a decrease in E_1 comparing *n*,*m*-C6, *n*,*m*-C(6 + 6) and *n*,*m*-C(6 + 6 + 6) for both 1,2 and 1,4 dicarbonyls. The same holds for 1,3-C4 and 1,3-C(4 + 4); however, the opposite trend is found in 1,2-C4 and 1,2-C(4 + 4). Regarding the size of the ring, an irregular behavior is observed in E_1, increasing from 1-C3 to 1-C5 but decreasing in 1-C7. We have also calculated the second reduction potential (E_2), see Table S9 and Figure S10 in the SI. Monocarbonyls range from 0.72 to 2.08 V, while dicarbonyls range from 0.74 to 2.67 V. The trends are the same as in the E_1.

Finally, we have studied the process of lithiation, described in Fig. 10, since carbonyl compounds undergo redox reactions during the charging and discharging processes and interact with Li when they are used as electrode materials in lithium-ion batteries. This methodology has been previously used in the literature [111]

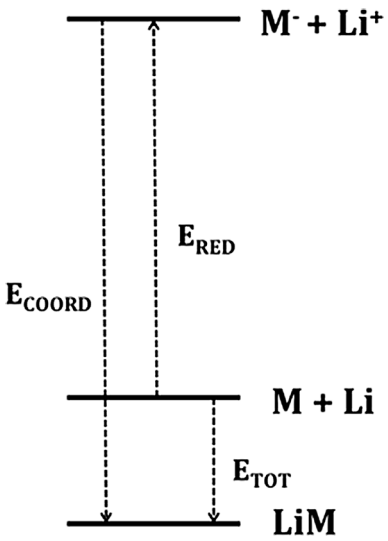

Fig. 10 Lithiation mechanism in the charge/discharge process in a lithium-ion battery

and allows a better characterization of the redox properties of these molecules. The following three parameters, reduction energy (E_{RED}), coordination energy (E_{COOR}) and total energy (E_{TOT}), are defined as:

$$E_{RED} = E(M^-) + E(Li^+) - (E(M) + E(Li))$$
$$E_{COOR} = E(LiM) - (E(M^-) + E(Li^+))$$
$$E_{TOT} = E(LiM) - (E(M) + E(Li))$$

In Fig. 10, the values of the total binding energy (E_{TOT}) together with the diradical character are represented. In Table S10 of the Supporting Information are collected the numerical values for E_{COOR}, E_{RED} and E_{TOT}. Inspecting the monocarbonyl compounds, very similar coordination energies (E_{COORD}) are obtained, ranging from −5.88 to −6.49 eV, revealing that the reduction energy (E_{RED}) is the main responsible of the observed pattern in the binding energies (E_{TOT}). On the other hand, this feature is not observed in the dicarbonyl compounds, as expected, since the relative position of the carbonyl moieties will affect the interaction with Li^+. This dependence of the binding energy on the position of the carbonyl groups is recognized in Fig. 11, where molecules with neighboring carbonyls tend to show higher coordination energies, as the lithium cation is located between both oxygen atoms. For instance, while for most of the anthraquinones, *n*,*m*-C(6 + 6 + 6), the coordination energies vary from −5.64 to −5.88 eV, this energy for 1,2- and 2,3-C(6 + 6 + 6) molecules amounts −7.15 and −7.02 eV, respectively. If the carbonyl groups are not adjacent but spatially close, some extra stabilization is gained favoring the reduced complex. This can be observed comparing 1,2- and 1,9-C(7 + 7), where the carbonyl oxygens are separated 2.81 and 4.80 Å, respectively, and the coordination energies are −7.13 and −6.35 eV, respectively. The latter is still greater than the energies of the rest of the *n*,*m*-C(7 + 7) molecules, which amount less than −6 eV.

It is not easy to establish a direct relationship between binding energy and diradical character. The binding energy depends on the reduction energy, which may be lowered with greater diradical character (due to larger electron affinities), but also on the anion–cation interaction, which is independent of the diradical character of the neutral species, and probably is the most relevant feature. Thus, we find some groups where larger diradical characters yield larger binding energies, such as *n*,*m*-C(4 + 6), *n*,*m*-C(4 + 4), *n*,*m*-C(4 + 6) and *n*,*m*-C(6 + 6 + 6) groups. However, in other groups the behavior of E_{TOT} is rather irregular.

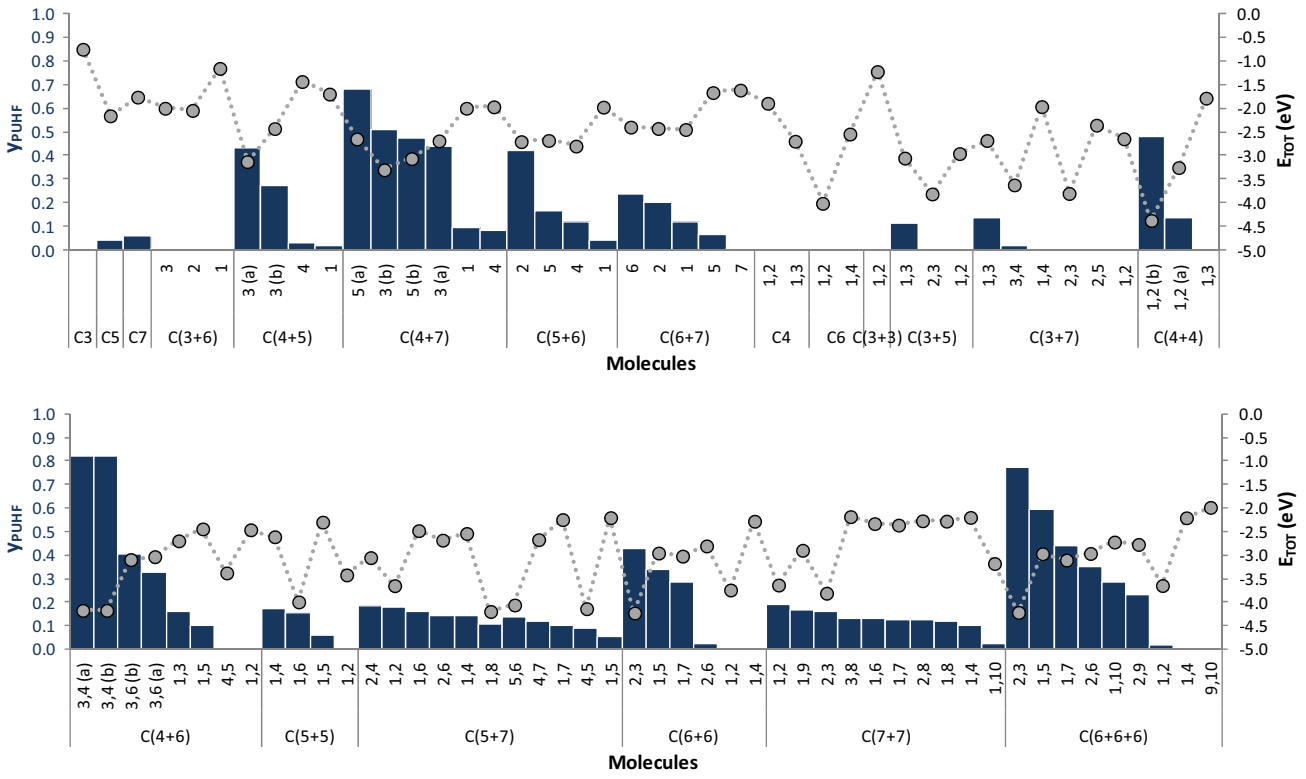

Fig. 11 Total binding energy (E_{TOT}), in eV, of the lithiation process and diradical character (y_{PUHF}) calculated at the B3PW91/aug-cc-pVTZ//B3PW91/6-31+G(*d*) level of theory

4 Conclusions

In this work, theoretical methods of quantum chemistry have been used for the investigation of the diradical character and molecular properties of a set of 90 conjugated carbonyls based on cyclic hydrocarbons. Molecular geometries, relative stability, aromaticity, singlet–triplet gaps, ionization energies, electron affinities, redox potentials and binding energies to lithium cation have been studied and analyzed in terms of the diradical character and structural features. We have found that, excluding the monocycles, many of the proposed molecules have a non-negligible diradical character and the ground state should be described as a singlet open-shell state. Some of the calculated parameters such as the spin density, bond distances and aromaticity show that the radical electrons are mainly delocalized over the carbon backbone. The diradical character is related to a larger instability and to a decrease in the aromaticity of the molecule.

From the analysis of the electron affinities (EA), the following trend may be devised: In those groups where several or all molecules show certain diradical character, this feature accomplishes larger EAs. Nevertheless, those molecules with closed-shell ground states may display large EAs too. With respect to the ionization energies (IE), no clear tendency is observed related to the diradical nature of the molecules, although in some cases large values of y_{PUHF} correspond to small IEs. We have also calculated the first (E_1) and second (E_2) redox potentials. Regarding E_1, we find the same trend as in the EAs, as expected, and molecules with large values of y_{PUHF} within a particular group yield larger redox potentials. On the other hand, as it was previously noted for the EAs, some closed-shell molecules also display large redox potentials. Besides, the number of fused rings decreases E_1 but, regarding the size of the ring, an irregular behavior is observed. Finally, we have studied the lithiation process, since the carbonyls interact with Li during the charge and discharge of the lithium-ion batteries. Regarding the monocarbonyls, the most relevant term is the reduction energy (E_{RED}), while in dicarbonyls the most important feature is the relative position of the carbonyls. No clear relationship of the total lithiation energy with the diradical character is observed, because the coordination energy depends on the carbonyl anion.

As a summary, this work highlights the singlet diradical nature shown by many conjugated cyclic carbonyl compounds, and the requirement to be properly described as singlet open-shell ground states, in contrast to the commonly assumed closed-shell nature. This feature, which has been neglected in almost all of the previously published works, has a considerable impact on molecular properties and suggests that the diradical character may be used as a new, unexplored variable, together with modifications of the backbone, for tuning redox potentials, a relevant characteristic in the design of new organic cathode materials.

Acknowledgements Technical and human support provided by IZO-SGI, SGIker (UPV/EHU, MICINN, GV/EJ, ERDF and ESF) is gratefully acknowledged for assistance and generous allocation of computational resources.

References

1. Anthony JE (2006) Chem Rev 106:5028
2. Bendikov M, Wudl F, Perepichka DF (2014) Chem Rev 104:4891
3. Mishra A, Bäuerle P (2012) Angew Chem Int Ed 51:2020
4. Anthony JE (2008) Angew Chem Int Ed 47:452
5. Paci I, Johnson JC, Chen X, Rana G, Popovic D, David DE, Nozik AJ, Ratner MA, Michl J (2006) J Am Chem Soc 128:16546
6. Smith MB, Michl J (2010) Chem Rev 110:6891
7. Minami T, Nakano M (2012) J Phys Chem Lett 3:145
8. Di Motta S, Negri F, Fazzi D, Castiglioni C, Canesi V (2010) J Phys Chem Lett 1:3334
9. Ponce-Ortiz R, Casado J, Rodríguez-González S, Hernández V, López-Navarrete JT, Viruela PM, Ortí E, Takimiya K, Otsubo T (2010) Chem Eur J 16:470
10. Nakano M, Kishi R, Nitta T, Kubo T, Nakasuji K, Kamada K, Ohta K, Champagne B, Botek E, Yamaguchi K (2005) J Phys Chem A 109:885
11. Boratyński PJ, Pink M, Rajca S, Rajca A (2010) Angew Chem Int Ed 49:5459
12. Abe M (2013) Chem Rev 113:7011
13. Shimizu A, Tobe Y (2011) Angew Chem Int Ed 50:6906
14. Kawase T, Ueno N, Osa M (1992) Tetrahedron Lett 33:5405
15. Zhang K, Huang K-W, Li J, Chi C, Wu J (2009) Org Lett 11:4854
16. Chase DT, Fix AG, Rose BD, Weber CD, Nobusue S, Stockwell CE, Zakharov LN, Lonergan MC, Haley MM (2011) Angew Chem Int Ed 50:11103
17. Chase DT, Rose BD, McClintock SP, Zakharov LN, Haley MM (2011) Angew Chem Int Ed 50:1127
18. Rose BD, Vonnegut CL, Zakharov LN, Haley MM (2012) Org Lett 14:2426
19. Reta-Mañeru D, Pal AK, Moreira IPR, Datta SN, Illas F (2014) J Chem Theory Comput 10:335
20. Saito T, Nishihara S, Yamanaka S, Kitagawa Y, Kawakami T, Yamada S, Isobe H, Okumura M, Yamaguchi K (2011) Theor Chem Acc 130:739
21. Nakamura T, Gagliardi L, Abe M (2010) J Phys Org Chem 23:300
22. Cramer CJ (1998) J Am Chem Soc 120:6261
23. Li X, Paldus J (2008) J Theor Comput Chem 7:805
24. Casado J, Ponce-Ortiz R, López-Navarrete JT (2012) Chem Soc Rev 41:5672
25. Lopez X, Ruipérez F, Piris M, Matxain JM, Ugalde JM (2011) ChemPhysChem 12:1061
26. Lopez X, Piris M, Matxain JM, Ruipérez F, Ugalde JM (2011) ChemPhysChem 12:1673
27. Sun Z, Zeng Z, Wu J (2014) Acc Chem Res 47:2582

28. Yang H, Song Q, Li W, Song X, Bu Y (2012) J Phys Chem C 116:5900
29. Romanova J, Liégeois V, Champagne B (2014) Phys Chem Chem Phys 16:21721
30. Minami T, Nakano M (2013) J Phys Chem A 117:2000
31. Song Z, Zhou H (2013) Energy Environ Sci 6:2280
32. Liang Y, Tao Z, Chen J (2012) Adv Energy Mater 2:742
33. Song Z, Zhan H, Zhou Y (2009) Chem Commun 4:448
34. Chen H, Armand M, Courty M, Jiang M, Grey CP, Dolhem F, Tarascon JM, Poizot P (2009) J Am Chem Soc 131:8984
35. Choi W, Harada D, Oyaizu K, Nishide H (2011) J Am Chem Soc 133:19839
36. Zhou W, Hernández-Burgos K, Burkhardt SE, Qian H, Abruña HD (2013) J Phys Chem C 117:6022
37. Genorio B, Pirnat K, Cerc-Korosec R, Dominko R, Gaberseck M (2010) Angew Chem Int Ed 49:7222
38. Namazian M, Coote ML (2007) J Phys Chem A 111:7227
39. Zhu X-Q, Wang C-H (2010) J Org Chem 75:5037
40. Pakiari AH, Siahrostami S, Mohajeri A (2008) Theochem 870:10
41. Namazian M, Siahrostami S, Noorbala MR, Coote ML (2006) Theochem 759:245
42. Cheng J, Sulpizi M, Sprik M (2009) J Chem Phys 131:154504
43. Tobias Johnsson Wass JR, Ahlberg A, Panas I, Schiffrin DJ (2006) J Phys Chem A 110:2005
44. Hernández-Burgos K, Burkhardt SE, Rodríguez-Calero GG, Hennig RG, Abruña HD (2014) J Phys Chem C 118:6046
45. Beheshti A, Norouzi P, Ganjali MR (2012) Int J Electrochem Sci 7:4811
46. Yao M, Senoh H, Araki M, Sakai T, Yasuda K (2010) ECS Trans 28:3
47. Er S, Suh C, Marshak MP, Aspuru-Guzik A (2015) Chem Sci 6:885
48. Bachman JE, Curtiss LA, Assary RS (2014) J Phys Chem A 118:8852
49. Assary RS, Brushett FR, Curtiss LA (2014) RSC Adv 4:57442
50. Kim KC, Liu T, Lee SW, Jang SS (2016) J Am Chem Soc 138:2374
51. Hohenberg P, Kohn W (1964) Phys Rev 136:B864
52. Kohn W, Sham LJ (1965) Phys Rev 140:A1133
53. Becke AD (1993) J Chem Phys 98:5648
54. Perdew JP (1991) In: Ziesche P, Eschig H (eds) Electronic structure of solids '91. Akademie Verlag, Berlin, pp 11–20
55. Burke K, Perdew JP, Wang Y (1998) In: Dobson JF, Vignale G, Das MP (eds) Electronic density functional theory: recent progress and new directions. Plenum, New York, pp 81–121
56. Hehre WJ, Ditchfield R, Pople JA (1972) J Chem Phys 56:2257
57. Dunning TH (1989) J Chem Phys 90:1007
58. López-Carballeira D, Ruipérez F (2016) J Mol Model 22:76
59. Cossi M, Barone V, Cammi R, Tomasi J (1996) Chem Phys Lett 255:327
60. Barone V, Cossi M, Tomasi J (1997) J Chem Phys 107:3210
61. Cances E, Mennucci B, Tomasi J (1997) J Chem Phys 107:3032
62. Barone V, Cossi M, Tomasi J (1998) J Comput Chem 19:404
63. Henry DJ, Parkinson CJ, Radom L (2002) J Phys Chem A 106:7927
64. Izgorodina EI, Coote ML (2006) J Phys Chem A 110:2486
65. Gaussian 09, Revision A.1, Frisch MJ, Trucks GW, Schlegel HB, Scuseria GE, Robb MA, Cheeseman JR, Scalmani G, Barone V, Mennucci B, Petersson GA, Nakatsuji H, Caricato M, Li X, Hratchian HP, Izmaylov AF, Bloino J, Zheng G, Sonnenberg JL, Hada M, Ehara M, Toyota K, Fukuda R, Hasegawa J, Ishida M, Nakajima T, Honda Y, Kitao O, Nakai H, Vreven T, Montgomery Jr. JA, Peralta JE, Ogliaro F, Bearpark M, Heyd JJ, Brothers E, Kudin KN, Staroverov VN, Kobayashi R, Normand J, Raghavachari K, Rendell A, Burant JC, Iyengar SS, Tomasi J, Cossi M, Rega N, Millam JM, Klene M, Knox JE, Cross JB, Bakken V, Adamo C, Jaramillo J, Gomperts R, Stratmann RE, Yazyev O, Austin AJ, Cammi R, Pomelli C, Ochterski JW, Martin RL, Morokuma K, Zakrzewski VG, Voth GA, Salvador P, Dannenberg JJ, Dapprich S, Daniels AD, Farkas Ö, Foresman JB, Ortiz JV, Cioslowski J, Fox DJ (2009) Gaussian Inc., Wallingford CT
66. Noodleman L (1981) J Chem Phys 74:5737
67. Noodleman L, Baerends EJ (1984) J Am Chem Soc 106:2316
68. Noodleman J, Davidson ER (1986) J Chem Phys 109:131
69. Yamakana S, Okumura M, Nakano M, Yamaguchi K (1995) J Mol Struct 310:205
70. Nakano M, Kishi R, Nakagawa N, Ohta S, Takahashi H, Furukawa S, Kamada K, Ohta K, Champagne B, Botek E, Yamaguchi K (2006) J Phys Chem A 110:4238
71. Nakano M, Kishi R, Ohta S, Takebe A, Takahashi H, Furukawa S, Kubo T, Morita Y, Nakasuji K, Yamaguchi K, Kamada K, Ohta K, Champagne B, Botek E (2006) J Chem Phys 125:074113
72. Yamaguchi K, Takahara Y, Fueno T, Nasu K (1987) Jpn J Appl Phys 26:L1362
73. Yamaguchi K, Jensen F, Dorigo A, Houk KN (1988) Chem Phys Lett 149:537
74. Isse AA, Gennaro A (2010) J Phys Chem B 114:7894
75. Roos BO, Taylor PR, Siegbahn PEM (1980) Chem Phys 48:157
76. Siegbahn PEM, Heiberg A, Almlöf J, Roos BO (1981) J Chem Phys 74:2384
77. Siegbahn PEM, Heiberg A, Roos BO, Levy B (1980) Phys Scr 21:323
78. Andersson K, Malmqvist P-Å, Roos BO, Sadlej AJ, Wolinski K (1990) J Phys Chem 94:5483
79. Andersson K, Malmqvist P-Å, Roos BO (1992) J Chem Phys 96:1218
80. Aquilante F, De Vico L, Ferré N, Ghigo G, Malmqvist P-Å, Neogrády P, Pedersen TB, Pitoňák M, Reiher M, Roos BO, Serrano-Andrés L, Urban M, Veryazov V, Lindh R (2010) J Comput Chem 31:224
81. Ditchfield R (1974) Mol Phys 27:789
82. Wolinski K, Hilton JF, Pulay PJ (1990) J Am Chem Soc 112:8251
83. Schleyer PvR, Maerker C, Dransfeld A, Jiao H, Hommes NJRvE (1996) J Am Chem Soc 118:6317
84. Schleyer PvR, Manoharan M, Wang ZX, Kiran B, Jiao HJ, Puchta R, Hommes NJRvE (2001) Org Lett 3:2465
85. Corminboeuf C, Heine T, Seifert G, Schleyer PvR, Weber J (2004) Phys Chem Chem Phys 6:273
86. Gomes JANF, Mallion RB (2001) Chem Rev 101:1349
87. Bendikov M, Duong HM, Starkey K, Houk KN, Carter EA, Wudl F (2004) J Am Chem Soc 126:7416
88. Motomura S, Nakano M, Fukui H, Yoneda K, Kubo T, Carion R, Champagne B (2011) Phys Chem Chem Phys 13:20575
89. Fu Q, Yang J, Wang X (2011) J Phys Chem A 115:3201
90. Galaup JP, Megel J, Trommsdoff HP (1976) Chem Phys Lett 41:397
91. Lin ZP, Aue WA (2000) Spectrochim Acta A Mol Biomol Spectrosc 56A:111
92. Golas E, Lewars E, Liebman JF (2009) J Phys Chem A 113:9485
93. Tomerini D, Gatti C, Frayret C (2016) Phys Chem Chem Phys 18:2442
94. Nourmohammadian F, Yavari I, Mohtat B, Shafaei SZ (2007) Dyes Pigments 75:479
95. Yavari I, Zabarjad-Shiraz N (2007) Dyes Pigments 75:669
96. Szatylowicz H, Krygowski TM, Solà M, Palusiak M, Dominikowska J, Stasyuk OA, Poater J (2015) Theor Chem Acc 134:35

97. PvR Schleyer (2001) Chem Rev 101:1115
98. Hückel E (1937) Z Elektrochem 43:827
99. Heinis T, Chowdhury S, Scott SL, Kebarle P (1988) J Am Chem Soc 110:400
100. Tozer DJ, de Proft F (2005) J Phys Chem A 109:8923
101. Kubo T, Shimizu A, Sakamoto M, Uruichi M, Yakushi K, Nakano M, Shiomi D, Sato K, Takui T, Morita Y, Nakasuji K (2005) Angew Chem Int Ed 44:6564
102. Kubo T, Sakamoto M, Nakasuji K (2005) Polyhedron 24:2522
103. Kubo T, Shimizu A, Uruichi M, Yakushi K, Nakano M, Shiomi D, Sato K, Takui T, Morita Y, Nakasuji K (2007) Org Lett 9:81
104. Lauer G, Schäfer W, Schweig A (1975) Chem Phys Lett 33:312
105. Millefiori S, Gulino A, Casarin M (1990) J Chim Phys 87:317
106. Potapov VK, Sorokin VV (1971) High Energy Chem 5:435
107. Rothgery EF, Holt RJ, McGee HA Jr (1975) J Am Chem Soc 97:4971
108. Koenig T, Smith M, Snell W (1977) J Am Chem Soc 99:6663
109. Peover ME (1962) J Chem Soc 1962:4540
110. Scott LT (1983) Pure Appl Chem 55:363
111. Nokami T, Matsuo T, Inatomi Y, Hojo N, Tsukagoshi T, Yoshizawa H, Shimizu A, Kuramoto H, Komae K, Tsuyama H, Yoshida J (2012) J Am Chem Soc 134:19694